Physics Letters A 382 (2018) 771–775

Contents lists available at ScienceDirect

Physics Letters A

www.elsevier.com/locate/pla

Probability evolution method for exit location distribution

Jinjie Zhu, Zhen Chen, Xianbin Liu *

State Key Laboratory of Mechanics and Control of Mechanical Structures, College of Aerospace Engineering, Nanjing University of Aeronautics and Astronautics, Nanjing 210016, China

ARTICLE INFO

Article history:
Received 28 November 2017
Received in revised form 23 January 2018
Accepted 23 January 2018
Available online 31 January 2018
Communicated by C.R. Doering

Keywords:
Large deviation
Exit location distribution
Monte Carlo simulation

ABSTRACT

The exit problem in the framework of the large deviation theory has been a hot topic in the past few decades. The most probable escape path in the weak-noise limit has been clarified by the Freidlin–Wentzell action functional. However, noise in real physical systems cannot be arbitrarily small while noise with finite strength may induce nontrivial phenomena, such as noise-induced shift and noise-induced saddle-point avoidance. Traditional Monte Carlo simulation of noise-induced escape will take exponentially large time as noise approaches zero. The majority of the time is wasted on the uninteresting wandering around the attractors. In this paper, a new method is proposed to decrease the escape simulation time by an exponentially large factor by introducing a series of interfaces and by applying the reinjection on them. This method can be used to calculate the exit location distribution. It is verified by examining two classical examples and is compared with theoretical predictions. The results show that the method performs well for weak noise while may induce certain deviations for large noise. Finally, some possible ways to improve our method are discussed.

1. Introduction

Noise is usually considered to be annoying and may be ignored in most of the cases. However, during the past few decades, it has exhibited incredible roles on the phenomena of stochastic resonance (SR) [1] and coherence resonance (CR) [2], which has aroused broad interest in a variety of disciplines. SR shows that under some certain strength of noise, the amplitude of the external signal can be significantly enhanced. On the other hand, even for arbitrarily small noise, the response can be carried away from the asymptotic stable equilibrium position for sufficiently large time [3]. The latter can be of great relevance to the reliability of engineering structures on the problem of first passage failure [4]. In the framework of large deviation theory, Freidlin and Wentzell [3] applied the concept of action functional attached to each sample path to investigate the exit problem. They showed that in the weak-noise limit, the exit from a domain must take place along an extremal of the action functional with overwhelming probability. In other words, for sufficiently small noise, the escape paths rarely happen, but when they escape, the paths escape with high probability along the pathway that is least unlikely. That makes rare events predictable and noise less noisy. This elegant theory has also been verified by abundant experiments by Dykman, McClintock and their coworkers [5–7].

To accurately depict the whole exit process, the probability density function, which is the solution of the corresponding Fokker–Planck–Kolmogorov (FPK) equation, should be solved. This is not always an easy task even for low dimensional dynamical systems. Analytical results can only be obtained under some restrict circumstances, e.g. detailed balance or generalized stationary potential [8]. Thus, other approximation methods should be introduced to uncover some characteristics of a specific exit problem. These characteristics include most probable escape path (MPEP), mean first passage time (MFPT), exit location distribution (ELD), etc. Dykman et al. [5] defined the prehistory probability density to describe the distribution of paths ending at the final state from which they evolve the system backwards in time. The ridge along the top of the distribution of this quantity corresponds to the MPEP of the given system. The action plot method [9] is introduced by Beri et al. which is actually a topological method which enumerates the trajectories starting from a small neighboring area of the initial position. The trajectory with least action will be chosen as the MPEP. Other methods such as the geometric minimum action method (gMAM) [10] and the ordered upwind method (OUM) [11] are also very efficient in calculating the MPEP. These methods have been shown for accuracy and consistency in the excitable system [12]. In real physical systems, the noise strength cannot be arbitrarily small. The MPEP and ELD may be modified for finite noise inten-

* Corresponding author.
E-mail address: xbliu@nuaa.edu.cn (X. Liu).

https://doi.org/10.1016/j.physleta.2018.01.027
0375-9601/

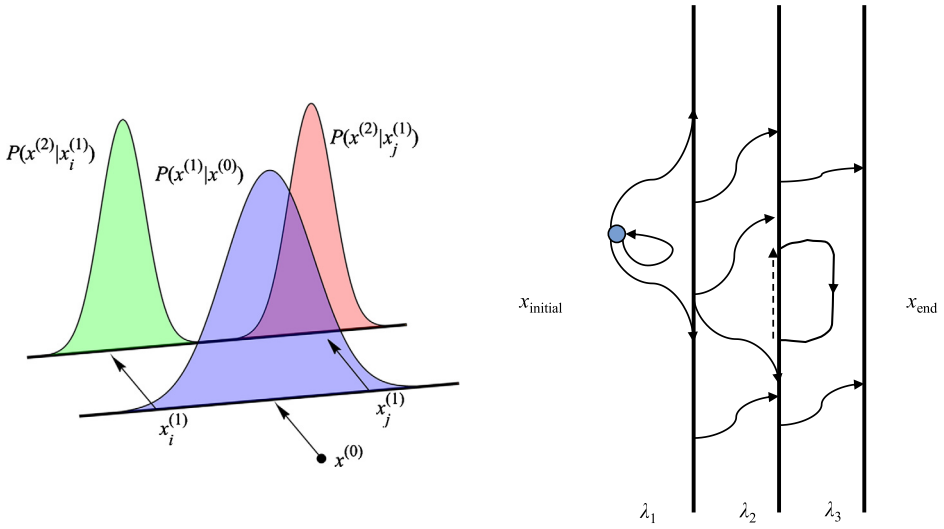

Fig. 1. Illustration of the probability evolution method. Left panel: the probability evolution example. The superscript represents the label of the interface and the subscript represents the point on the interface. The blue, green and red patches represent the transition probability distribution from the point in the previous interface to the next interface. Right panel: the sampling paths between the interfaces λ_i. The dashed arrow represents the reinjection. Details are in the text. (For interpretation of the references to color in this figure legend, the reader is referred to the web version of this article.)

sities, e.g. noise-induced shift [13,14] and saddle-point avoidance [15].

To obtain the exit location distribution for finite noise strengths, if the explicit theoretical expression cannot be calculated, direct Monte Carlo (brute force) simulation may be a good candidate which first comes to one's mind. However, when noise is small enough, the MFPT grows exponentially as noise approaches zero [16]. As a matter of fact, one is forced to waste considerable time on uninteresting dynamical behaviors until the final escape happens. Researchers have been looking for methods to accelerate the process. In order to speed up the sampling process, Allen et al. [17] presented the forward flux sampling (FFS) technique first applying in biochemical networks. This method employs several nonintersecting interfaces in phase space between the initial and final states and generates rare paths in a ratchetlike manner [18]. By using similar ideas, the barrier method [19] and milestoning [20–23] also apply interfaces to accelerate simulations. Glowacki et al. [24] introduced an even simpler method named boxed molecular dynamics which can efficiently calculate the free energy profiles. These methods are very popular in molecular dynamics (MD) simulations. Based on the knowledge of the MPEP in theory in the weak-noise limit, Beri et al. [14] used the dynamic importance sampling (DIMS) to keep the trajectory on the stable manifold of the MPEP whenever the trajectory leaves a small neighborhood of it. Crooks and Chandler [25] realized another side of the coin by directly sampling the noise process. Recently, Han et al. [26] applied the generalized cell mapping (GCM) method to the exit location distribution problem which showed quite satisfactory agreement between the theory and numerical simulation.

In this paper, we propose a method named as probability evolution method (PEM) to calculate the ELD by combining the advantages of the FFS method and the fast Monte Carlo simulations used by Bandrivskyy et al. in Ref. [27]. The structure of this paper is as follows. In Section 2, the PEM is illustrated and is compared with previous methods. It is applied to two classical examples in Section 3 and is validated by theoretical results. Finally, discussions and conclusions are given in Section 4.

2. Method

As is in the FFS method, PEM also applies several nonintersecting interfaces between the initial (equilibrium points, limit cycles, chaotic attractors, etc.) and final (saddle points, limit cycles, chaotic saddles, etc.) states. Different to the FFS method, the calculation between different interfaces is independent and the sample paths are not necessary to be reserved. The detailed process goes as follows. We take the stable equilibrium point being the initial state as an example. As is in Fig. 1, we start N_1 samples from the equilibrium and only record the final position of the path at the first interface λ_1. The transition probability distribution (TPD) can be calculated as $P\left(x^{(1)}|x^{(0)}\right)$ (the superscripts represent the label of the interfaces). By starting N_{i+1} samples at each point of the interface λ_i, say the kth point $x_k^{(i)}$, for each sample, whenever the path crosses λ_i due to relaxation, it will be reinjected back to the initial position $x_k^{(i)}$ [see the dashed arrow in Fig. 1]. As above, the final position of the path at λ_{i+1} will be recorded. The TPDs for all the points from λ_i to λ_{i+1} can be obtained as $P\left(x^{(i+1)}|x^{(i)}\right)$. Note that $P\left(x^{(i+1)}|x^{(i)}\right)$ is a matrix and each row is a TPD of a point in λ_i to the interface λ_{i+1}. By using the reinjection, the time cost for a point to reach the next interface or boundary can be reduced by an exponentially large factor as stated in Ref. [27]. It should be remarked that this manipulation will induce errors since paths may go across the interface several times before they finally reach the next one. However, for small noise intensities, the error can be reduced because paths other than the MPEP shrink as the noise intensity decreases. In other words, the dispersion of the prehistory probability density shrinks with the decreasing noise [5,28,29]. In the end, the TPD from the initial to final state is obtained as follows:

$$P\left(x^{(\text{end})}|x^{(0)}\right) = \prod_{i=0}^{n} P\left(x^{(i+1)}|x^{(i)}\right) \tag{1}$$

where n is the number of the interfaces while $i = 0$ and $i = n + 1$ represent the initial and final states, respectively.

Apart from the reduction of the time cost by an exponentially large factor, the direct advantage of this method is the independence of the calculation for the TPD between different interfaces and between different points. It's the most essential difference between FFS and PEM, whereby for the former, the sample paths are allowed to step across the previous interface without the reinjection and the sample paths are fully recorded. So for FFS, the recorded information is the whole pathway. While for PEM, the

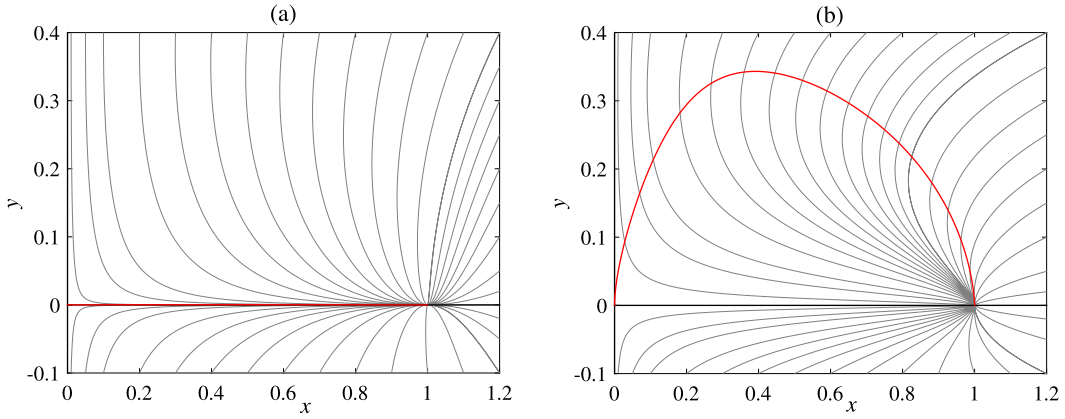

Fig. 2. The MPEP (red line) and the flow lines of the deterministic vector field (grey lines) for the Maier–Stein system. Parameters are (a) $\alpha = 6.67$, $\mu = 2$ and (b) $\alpha = 10$, $\mu = 0.67$. (For interpretation of the references to color in this figure legend, the reader is referred to the web version of this article.)

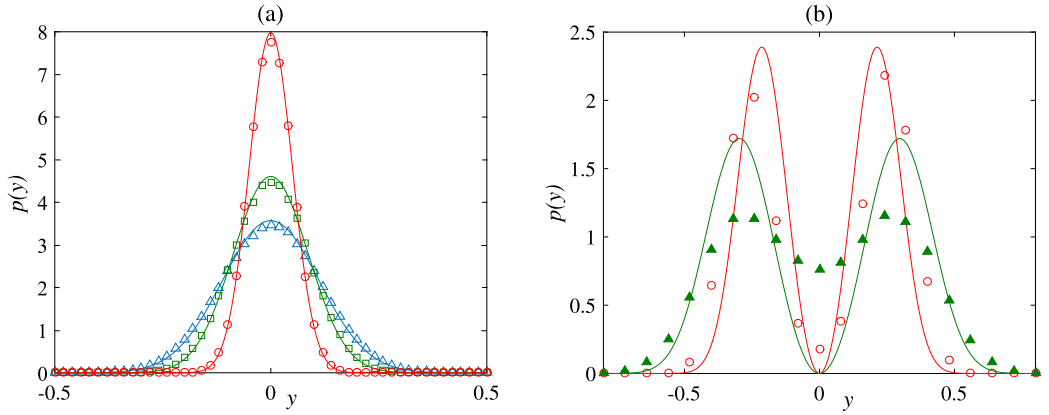

Fig. 3. Exit location distribution of the Maier–Stein system for different parameters by PEM. Solid lines are corresponding theoretical results. (a) $\alpha = 6.67$, $\mu = 2$. Noise strengths are $D = 0.05$ (blue triangle), 0.03 (green square), 0.01 (red cycle). The numbers of interfaces are 4, 5, 10, respectively and 10000 samples are issued from each point. (b) $\alpha = 10$, $\mu = 0.67$. Noise strengths are $D = 0.04$ (green triangle), 0.015 (red cycle). The numbers of interfaces are 1, 2, respectively and 5000 samples are issued from each point. (For interpretation of the references to color in this figure legend, the reader is referred to the web version of this article.)

recorded information is the starting and ending position at the interfaces. As a result, FFS can be used to compute the escape rate or MFPT while PEM can't. But it can be seen that for obtaining the same number of exit paths, PEM is more efficient because of the reinjection. Our method is also similar to the barrier method and the milestoning in that they all don't allow backtracking unlike the FFS method. In the barrier method, the avoidance of backtracking is realized by using the "jump" [19] when the previous barrier is reached and a closest lookup is added to move back to the current barrier to continue the trajectory. In the traditional milestoning method [20–22], backtracking is eliminated by using the reinitialization whenever the two neighboring milestones are reached. In PEM, the reinjection is more direct which don't allow paths to cross the current interface (barrier, milestone). Similarly, milestoning with Voronoi tessellations [23] and boxed molecular dynamics [24] employed the velocity inversion to restrict the trajectory inside the Voronoi cell and the box which are very meaningful in the molecular dynamics sense. Different to the "reflecting" of the milestoning with Voronoi tessellations and the boxed molecular dynamics, PEM directly pulls the path back to its initial position on the interface. In the next section, we will apply PEM to two classical systems to verify its effectiveness in calculating ELD.

3. Examples

In this section, the Maier–Stein system and the inverted Van der Pol oscillator (IVDP) are investigated by PEM and the results are compared with theoretical predictions.

3.1. Maier–Stein system

The Maier–Stein system is first proposed by Maier and Stein [16,30,31] which deals with the motion of an overdamped particle in the two dimensional drift vector field. Since the analytical results of the ELDs have been obtained in Ref. [32], we can validate our numerical results by theoretical ones. The governing equations are as follows:

$$\begin{aligned} \dot{x} &= x - x^3 - \alpha x y^2 + \xi_1(t) \\ \dot{y} &= -\mu y\left(1 + x^2\right) + \xi_2(t) \\ \left\langle \xi_i(t) \right\rangle &= 0, \left\langle \xi_i(t)\, \xi_j(t-\tau) \right\rangle = D\delta_{ij}\delta(\tau). \end{aligned} \tag{2}$$

The vector field is not a gradient of a potential unless $\alpha = \mu$. The variable D represents the strength of the two isotropic Gaussian white noises. We consider two sorts of parameters, namely, $\alpha = 6.67$, $\mu = 2$ and $\alpha = 10$, $\mu = 0.67$. The MPEPs for them are calculated by using gMAM [10] as in Fig. 2.

For Fig. 2(a), the MPEP follows the x-axis from the stable equilibrium $(1, 0)$ to the saddle point $(0, 0)$. It resembles the case of unbroken symmetry [31] and the MPEP is a time-reversed relaxational trajectory which is tangent to the x-axis. The theoretical ELD on the y-axis follows $P(y) = \left(\frac{2}{\pi D}\right)^{1/2} \exp\left(-\frac{2y^2}{D}\right)$ (solid lines in Fig. 3(a)) [25,31]. This is a well-defined Gaussian distribution. By numerical simulations of PEM, the ELDs for three noise intensities are computed ($D = 0.05, 0.03$ and 0.01). It can be seen in Fig. 3(a),

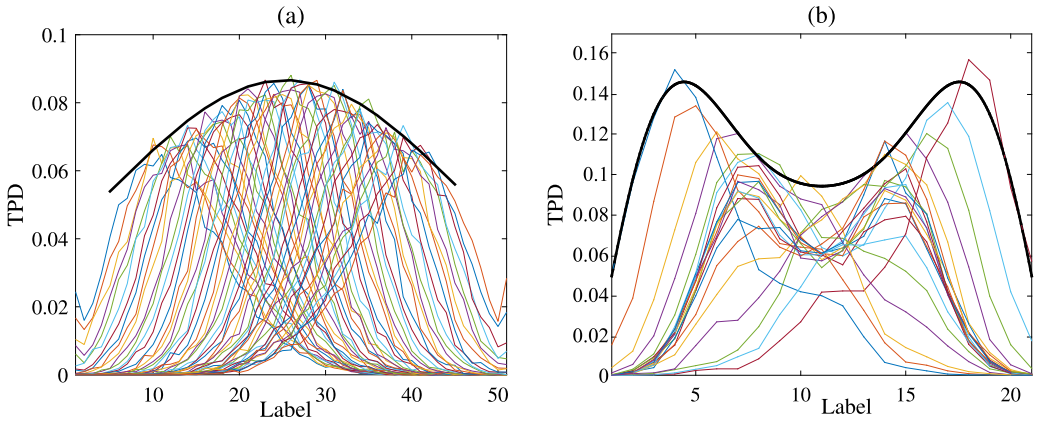

Fig. 4. The transition probability distributions (TPD) of a pair of the interfaces in the Maier–Stein system. The bold black curves represent the envelopes of the TPDs. Parameters are (a) $\alpha = 6.67$, $\mu = 2$, $D = 0.05$. 51 points are used at each interface in the interval $y = [-0.5, 0.5]$. The TPDs are calculated from the 3th to the 4th interface. (b) $\alpha = 10$, $\mu = 0.67$, $D = 0.04$. 21 points are used at each interface in the interval $y = [-0.8, 0.8]$. The TPDs are calculated from the 1th to the 2th interface. (For interpretation of the references to color in this figure legend, the reader is referred to the web version of this article.)

with the decrease of the noise strength, the width of the distribution shrinks and the height increases. This is an evidence for the escape location concentrating at the saddle point which is consistent with the result of the weak-noise limit that MPEP will escape though the saddle. The results of PEM perform well compared with the theoretical ones. For Fig. 2(b), the MPEP approaches saddle point asymptotically along the y-axis. It is intuitive by considering the Wentzel–Kramers–Brillouin (WKB) approximation that since the MPEP curve is tangent to the y-axis, the WKB tube will touch the y-axis before the MPEP crosses the saddle. This explains the saddle-point avoidance observed in Ref. [15]. Due to the symmetric property, the ELD will be a symmetric bimodal Weibull distribution as the noise intensity approaches zero [15,25,32]. The theoretical ELD reads $P(y) = \left(\frac{2}{A^{2/\mu} D\mu}\right) |y|^{2/\mu - 1} \exp\left(-(|y|/A)^{2/\mu}/D\right)$, where A is the limit of y/x^{μ}. Note that the theoretical ELD is valid only in the weak-noise limit, so the unsatisfactory disagreement between the theoretical and numerical results can be foreseen. But the phenomenon of saddle-point avoidance and the tendency for the coincidence between the theoretical and numerical ELDs have shown the effectiveness of PEM.

The TPD matrix between interfaces can reveal some fluctuation properties which may shed some lights on the final ELD. For the two parameter cases in Fig. 3(a)–(b), we plot the TPDs between one pair of the interfaces for $D = 0.05$ in Fig. 3(a) and $D = 0.04$ in Fig. 3(b). The results are in Fig. 4. As we can see, the unimodal envelope of the TPDs in Fig. 4(a) and the bimodal envelope of the TPDs in Fig. 4(b) are consistent with the ELDs in Fig. 3(a) and Fig. 3(b), respectively.

3.2. Inverted Van der Pol oscillator

The inverted Van der Pol oscillator has been considered in Ref. [9,14]. It has an unstable limit cycle and a stable equilibrium point. The system is described by the following equations:

$$\begin{aligned} \dot{x} &= y \\ \dot{y} &= -x - 2\eta\left(1 - x^2\right) y + \sqrt{\varepsilon}\xi(t) \end{aligned} \tag{3}$$

The variable ε represents the strength of the noise and $\langle \xi(t)\xi(t-\tau)\rangle = \delta(\tau)$. Note that noise only appears on the right hand side of the second equation, so it is actually not isotropic. The variable η controls the size of the unstable limit cycle. In this paper, we fix $\eta = 0.5$. For different noise intensities, ELDs on the limit cycle can be obtained by using PEM. The results are in Fig. 5. We can see that the peaks shifted with the decrease of the noise. The

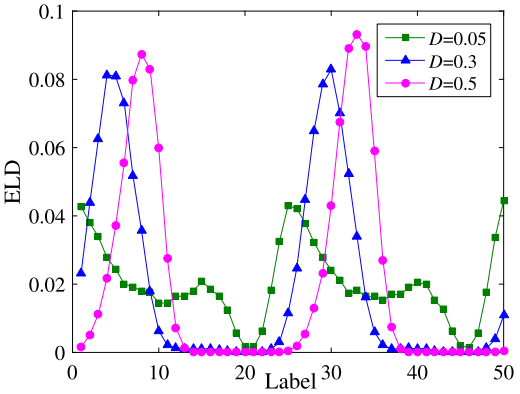

Fig. 5. The exit location distribution (ELD) of the inverted Van der Pol oscillator (IVDP) for different noise intensities.

symmetric structure of the ELD (two peaks) is a natural result of the central symmetric property of the IVDP system. The widening of the distribution as the noise decreases can be observed which can be explained as follows. As noise strength approaches zero, the MPEP will be a heteroclinic trajectory connects the stable equilibrium point and the unstable limit cycle which is tangent to the limit cycle. Thus, the ELD will be close to a uniform distribution.

To compare the theoretical and numerical results, we consider the correction of the action functional $S_{\varepsilon} = S - \varepsilon \ln(z)$ [13,14], where ε is the strength of the finite noise and z is the prefactor term in the WKB approximation. Fig. 6 shows the results of the theory and numeric. We can see that as noise decreases, the numerical result (the green square) agrees well with the theory (the green line) while as noise strength increases ($D = 0.3$ and 0.5), their deviation increases. The source of the deviation has been explained in Section 2 which is a direct result of the reinjection process. Fortunately, the deviation can be reduced as noise decreases which meets our original intention of using PEM. We will further discuss this issue in Section 4.

4. Discussions and conclusions

In this paper, the probability evolution method is introduced which uses several interfaces between the initial and final states and applies the reinjection on them. The PEM can reduce the simulation time by an exponentially large factor which is essential when noise strength is small enough. This method can be used

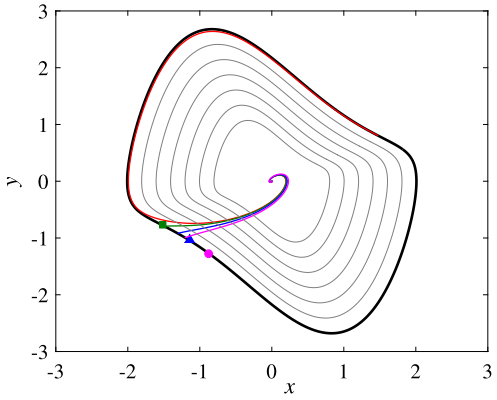

Fig. 6. The comparison of the theoretical noise-induced shift of the MPEPs and the numerical exit locations. The thick black line is the unstable limit cycle and the thin grey lines are interfaces used in PEM. The red line represents the MPEP in the weak-noise limit. The green square, blue triangle and pink circle are peaks of the ELDs for noise strengths $D = 0.05$, 0.3 and 0.5 in Fig. 5 and the lines of the same colors corresponding to them are the corrected MPEPs in theory. (For interpretation of the references to color in this figure, the reader is referred to the web version of this article.)

to calculate the ELD on the exit boundary and has been verified by examining the Maier–Stein system and the inverted Van der Pol oscillator. It performs well for weak noise but may induce some deviations for large noise. The deviation is caused by the operation of the reinjection. This deviation can be reduced for small noise as has been shown in Fig. 6. It can be explained that as the noise decreases, trajectories other than the MPEP in the weak-noise limit will be exponentially reduced, so that the reinjection will make less influence on the statistic of the TPDs between the interfaces.

Apart from the considerable reduction of the simulation time, the PEM is also good at saving memory. The recorded information is merely the starting and the ending position at the interfaces. In addition, the TPDs calculated from every point at the interface are independent between the points, so parallel computation can be applied to further reduce the time cost of the total simulation.

Despite the benefit of the reinjection, the deviation caused by this manipulation is another side of the double-edged sword. We hope to solve this problem to make the PEM more robust in the future. Taking into account of the mechanism of the deviation, there are two directions to be attempted at. First, the number of the interfaces may be decreased to reduce the error. In that case, the problem is how many interfaces are proper for noise with a certain intensity and how large the deviation can we endure. The limit situation is that no interface will be used which is the same as the traditional Monte Carlo simulation. Second, the trajectories may be allowed to cross the interface backward to some extent. For example, the barrier method and the traditional milestoning method allow the path to cross the interface until the previous one. The question is to what extent the deviation can be well reduced. The limit situation is no restriction on the crossing of the interface which will correspond to the FFS method. In any case, the PEM can be a suitable candidate to the weak noise case which is consistent with our intention.

Acknowledgements

This research was supported by the National Natural Science Foundation of China (Grants No. 11772149, No. 11472126 and No. 11232007) and the Project Funded by the Priority Academic Program Development of Jiangsu Higher Education Institutions (PAPD).

References

[1] L. Gammaitoni, P. Hänggi, P. Jung, F. Marchesoni, Rev. Mod. Phys. 70 (1998) 223.
[2] A.S. Pikovsky, J. Kurths, Phys. Rev. Lett. 78 (1997) 775.
[3] M. Freidlin, A.D. Wentzell, Random Perturbations of Dynamical Systems, Springer Science & Business Media, 2012.
[4] L. Chen, W. Zhu, Sci. China, Technol. Sci. 53 (2010) 2495–2500.
[5] M. Dykman, P.V. McClintock, V. Smelyanski, N. Stein, N. Stocks, Phys. Rev. Lett. 68 (1992) 2718.
[6] M. Dykman, D. Luchinsky, P.V. McClintock, V. Smelyanskiy, Phys. Rev. Lett. 77 (1996) 5229.
[7] D. Luchinsky, R. Maier, R. Mannella, P.V. McClintock, D. Stein, Phys. Rev. Lett. 79 (1997) 3109.
[8] Y.K.M. Lin, G.Q. Cai, Probabilistic Structural Dynamics: Advanced Theory and Applications, McGraw-Hill, New York, 1995.
[9] S. Beri, R. Mannella, D.G. Luchinsky, A. Silchenko, P.V. McClintock, Phys. Rev. E 72 (2005) 036131.
[10] M. Heymann, E. Vanden-Eijnden, Commun. Pure Appl. Math. 61 (2008) 1052–1117.
[11] M. Cameron, Phys. D: Nonlinear Phenom. 241 (2012) 1532–1550.
[12] Z. Chen, J. Zhu, X. Liu, in: Proc. R. Soc. A, The Royal Society, 2017, 20170058.
[13] A. Bandrivskyy, S. Beri, D. Luchinsky, Phys. Lett. A 314 (2003) 386–391.
[14] S. Beri, R. Mannella, P.V. McClintock, Phys. Rev. Lett. 92 (2004) 020601.
[15] D. Luchinsky, R. Maier, R. Mannella, P.V. McClintock, D. Stein, Phys. Rev. Lett. 82 (1999) 1806.
[16] R.S. Maier, D.L. Stein, J. Stat. Phys. 83 (1996) 291–357.
[17] R.J. Allen, P.B. Warren, P.R. Ten Wolde, Phys. Rev. Lett. 94 (2005) 018104.
[18] R.J. Allen, D. Frenkel, P.R. ten Wolde, J. Chem. Phys. 124 (2006) 024102.
[19] D.A. Adams, L.M. Sander, R.M. Ziff, J. Chem. Phys. 133 (2010) 124103.
[20] A.K. Faradjian, R. Elber, J. Chem. Phys. 120 (2004) 10880–10889.
[21] A.M. West, R. Elber, D. Shalloway, J. Chem. Phys. 126 (2007) 04B608.
[22] E. Vanden-Eijnden, M. Venturoli, G. Ciccotti, R. Elber, J. Chem. Phys. 129 (2008) 174102.
[23] E. Vanden-Eijnden, M. Venturoli, J. Chem. Phys. 130 (2009) 194101.
[24] D.R. Glowacki, E. Paci, D.V. Shalashilin, J. Phys. Chem. B 113 (2009) 16603–16611.
[25] G.E. Crooks, D. Chandler, Phys. Rev. E 64 (2001) 026109.
[26] Q. Han, W. Xu, X. Yue, Chaos Solitons Fractals 87 (2016) 302–306.
[27] A. Bandrivskyy, S. Beri, D. Luchinsky, R. Mannella, P.V. McClintock, Phys. Rev. Lett. 90 (2003) 210201.
[28] J. Gómez-Ordoñez, J. Casado, M. Morillo, Phys. Rev. E 54 (1996) 2125.
[29] M. Morillo, J. Casado, J. Gómez-Ordónez, Phys. Rev. E 55 (1997) 1521.
[30] R.S. Maier, D.L. Stein, Phys. Rev. E 48 (1993) 931.
[31] R.S. Maier, D.L. Stein, Phys. Rev. Lett. 71 (1993) 1783.
[32] R.S. Maier, D.L. Stein, SIAM J. Appl. Math. 57 (1997) 752–790.